INTERACTION OF LASER RADIATION WITH MATTER. LASER PLASMA

Selective emission and luminescence of Er₂O₃ under intense laser excitation

V.M. Marchenko, L.D. Iskhakova, M.I. Studenikin

Abstract. **The microstructure of Er$_2$O$_3$ polycrystals synthesised by laser heating is studied. The synthesis of erbium silicate (Er$_2$SiO$_5$) layers was observed upon interaction of Er$_2$O$_3$ and SiO$_2$ melts. The dependences of the selective emission (SE) and luminescence spectra of Er$_2$O$_3$ polycrystals in the range 200–1700 nm on the intensity of laser-thermal (at the wavelength $\lambda = 10.6$ μm) and resonant laser ($\lambda \approx 975$ nm) excitation are investigated. The emission of heated Er$_2$O$_3$ polycrystals arises as a result of multiphonon relaxation of absorbed energy and is a superposition of the SE at the electronic-vibrational transitions of Er^{3+} ions and the thermal radiation of the crystal lattice. The shape of the SE spectra of Er$_2$O$_3$ polycrystals in the range 400–1700 nm almost does not change upon laser-thermal heating from 300 to 1500 K and subsequent cooling and corresponds to the absorption spectra of Er^{3+} ions. With increasing temperature, the thermal radiation intensity increases faster than the SE intensity, and the shape of the Er$_2$O$_3$ spectrum becomes closer to the calculated spectrum of a blackbody. The anti-Stokes luminescence spectra of Er^{3+} ions formed under intense laser excitation of the ^{4}I$_{11/2}$ level are explained by additional SE caused by heating of the crystal matrix due to the Stokes losses. A difference between the SE and luminescence spectra is observed at low intensities of resonant laser excitation and low temperatures, when only the Stokes luminescence occurs. The temperature dependences of the SE and luminescence spectra of Er$_2$O$_3$ upon laser excitation testify to the fundamental role played by the interaction of the electronic f-shell of Er^{3+} ions with crystal lattice vibrations in the processes of multiphonon radiative and nonradiative relaxation. The laser-thermal synthesis is promising for in-process variation of the chemical composition of rare-earth samples.**

Keywords: *Er$_2$O$_3$, laser-thermal synthesis, microstructure, laser spectroscopy, selective emission, luminescence, quantum electronics, microelectronics, thermophotovoltaics, hypersonic aerodynamics.*

1. Erbium oxide Er$_2$O$_3$ is applied in opto- and microelectronics [1–6], thermophotovoltaic generators [7–10], nuclear reactors [11–13], and hypersonic aerodynamics [14]. The luminescence spectra of Er$_2$O$_3$ correspond to the transitions

V.M. Marchenko, M.I. Studenikin A.M. Prokhorov General Physics Institute, Russian Academy of Sciences, ul. Vavilova 38, 119991 Moscow, Russia; e-mail: vmarch@kapella.gpi.ru, mstud-iof@yandex.ru;
L.D. Iskhakova Fiber Optics Research Centre, Russian Academy of Sciences, ul. Vavilova 38, 119333 Moscow, Russia;
e-mail: ldisk@fo.gpi.ru

between the energy states of the screened 4f^{11} electronic shell of Er^{3+} ions [1, 15, 16]. At increased temperatures, the Er^{3+} luminescence is quenched due to the multiphonon nonradiative relaxation [3, 4]. Of fundamental interest is to study the nature of Er$_2$O$_3$ thermal radiation [9, 17–19]. Heating Er$_2$O$_3$ above 900 K causes intense selective emission (SE) in the range 400–1700 nm with the bands corresponding to the transitions between the energy states of Er^{3+}. At $T = 1540 – 1873$ K, the spectral emissivity of the bands $J_{se}(\lambda, T) = I_{se}(\lambda, T)/I_{bb}(\lambda, T) \leqslant 0.6$ [$I_{se}(\lambda, T), I_{bb}(\lambda, T)$ are the intensities of the SE and thermal radiation (TR) of a blackbody] is higher than the emissivity of the pedestal, i.e., of the continuous spectrum of the crystal lattice [20].

The laser synthesis of refractory oxides is used for fabricating single- and polycrystalline samples, as well as for studying their microstructural, spectral-energy, and thermophysical characteristics [21–25]. In [26], the microstructure and transformation of the luminescence and SE spectra of Yb$_2$O$_3$ polycrystals were studied upon resonant laser and laser-thermal excitation.

In the present work, we experimentally study the microstructure of Er$_2$O$_3$ samples and the transformation of their SE spectra in the range 400–1700 nm upon laser heating at the wavelength $\lambda = 10.6$ μm up to the melting temperature $T_m = 2691$ K in comparison with the reflection and luminescence spectra upon intense laser excitation of the ^{4}I$_{11/2} \leftarrow ^4$I$_{15/2}$ transitions of Er^{3+} ions at $\lambda \approx 975$ nm.
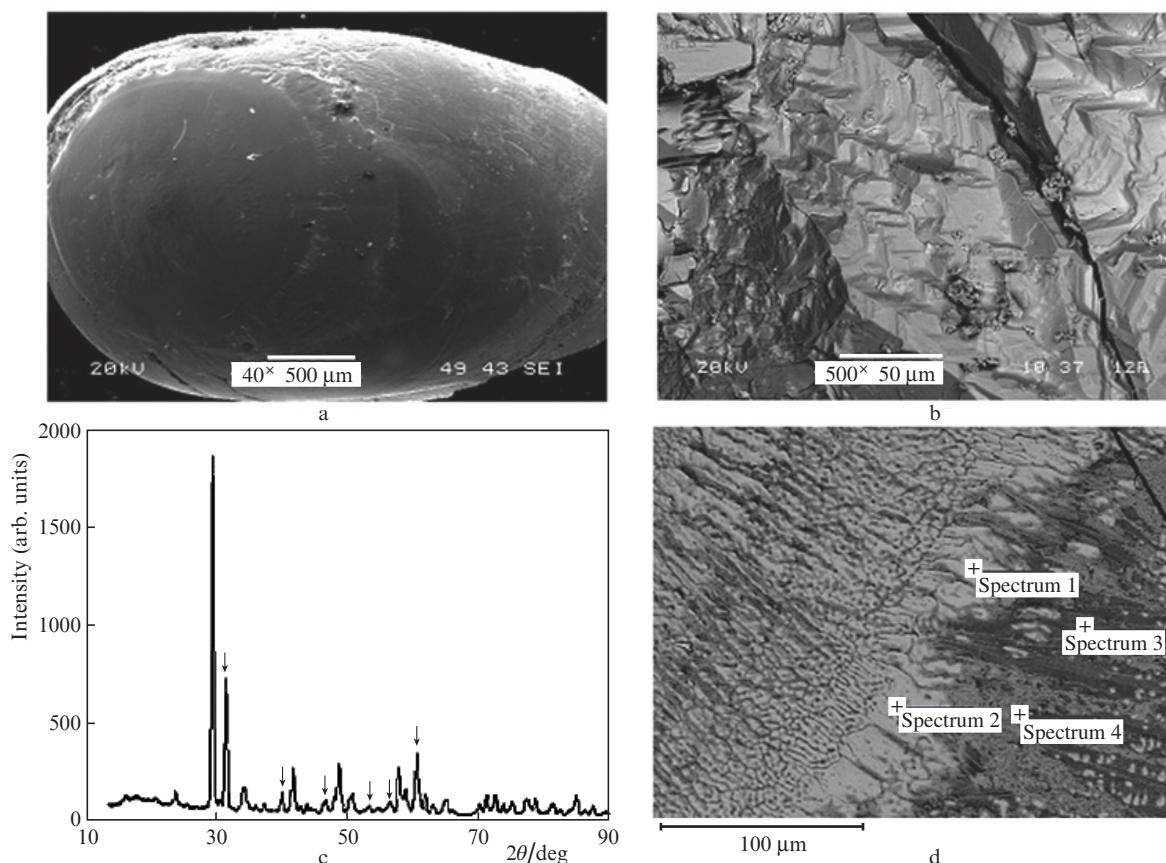
2. The Er$_2$O$_3$ samples were synthesised by melting powders of ultrahigh purity grade Itb0-1 (dispersion ability 1–50 μm) on a silicon substrate using an ILGN-709 cw CO$_2$ laser with the power $P_{las} < 100$ W and the wavelength $\lambda = 10.6$ μm at $T \geqslant T_m$. The samples were formed due to surface tension forces upon multiple melting and recrystallisation of the melt in air.

The study of the microstructure and the energy-dispersion micro-probe analysis of the elemental composition of the synthesised samples were performed on a JSM-5910LV electron microscope with an INCA ENERGY analytic system. The X-ray phase analysis was done using DRON-4-13 and D8 Discover diffractometers with GADDS (CuK$_\alpha$ radiation), at which we obtained the X-ray diffraction patterns of unbroken samples.

The shape (Fig. 1a) of the grown Er$_2$O$_3$ samples, as well as their chemical and phase composition depended on the synthesis conditions. The surface regions fused by a laser demonstrate ordered growth steps with a characteristic size of 5–40 μm (Fig. 1b), which testify to a microcrystalline structure of the Er$_2$O$_3$ samples synthesised by laser heating. Most of the samples had a single-phase cubic modification of Er$_2$O$_3$ (space group Ia-3, $Z = 16$), whose lattice constant was precisely

Figure 1. Microphotographs of an Er_2O_3 polycrystal synthesised by laser heating (a); growth steps of Er_2O_3 microcrystals (b); X-ray diffraction pattern of an Er_2O_3 sample with admixture of a hexagonal modification, whose reflections are marked by arrows (c); and interfaces between the Er_2O_3 (Spectrum 1 and Spectrum 2) and Er_2SiO_5 (Spectrum 3 and Spectrum 4) phases (d).

determined from the X-ray diffraction pattern to be $a =$ 10.5637(7) Å. The fused Er_2O_3 polycrystals have a low defect density [the angular width at half maximum for the (222) reflection is 0.16°]. Comparison of the X-ray diffraction patterns of the unbroken and powdered samples leads to the conclusion that the polycrystals have mainly the (001) texture. In some samples, we observed not only the stable cubic modification but also the hexagonal modification (Fig. 1c), which appeared as a result of phase transformation at $T = 2593$ K [27].

The study of the elemental and phase composition on the erbium oxide–quartz interface reveals the formation of erbium silicate Er_2SiO_5 in a chemical reaction occurring upon laser heating. From the Z-contrast image (Fig. 1d) and the microprobe analysis data, we can conclude that the crystallisation of Er_2O_3 in the light grey regions (denoted as Spectrum 1 and Spectrum 2 in Fig. 1d) occurs without formation of silicate, while the average atomic ratio in the dark regions (Spectrum 3 and Spectrum 4) is $Er : Si : O = 25.02 : 12.45 : 62.48$, which corresponds to the stoichiometry of Er_2SiO_5. The presence of the Er_2SiO_5 phase is also confirmed by the X-ray phase analysis.

3. The temperature dependence of the spatial intensity distribution of the emission of polycrystalline Er_2O_3 samples in the visible region upon laser-thermal excitation was experimentally studied using a Sony DSC-HX7V photo-video camera. The Er_2O_3 samples attached by melting to the face of a quartz rod 3 mm in diameter were heated during 30 s by a repetitively pulsed (0.66/20 ms) CO_2 laser with an average power of $\sim$2 W. The radiation intensity on the surface of

samples was varied by moving a NaCl lens with a focal length of 40 cm along the optical axis of the CO_2 laser. The surface temperature of Er_2O_3 polycrystals with a thermal radiation coefficient of 0.4 at $\lambda = 1$ μm [20] was measured by a 'Piton-104' pyrometer to be no higher than 1400 K. Figure 2 shows a set of frames (spaced by 5 s) of the transformation of the SE
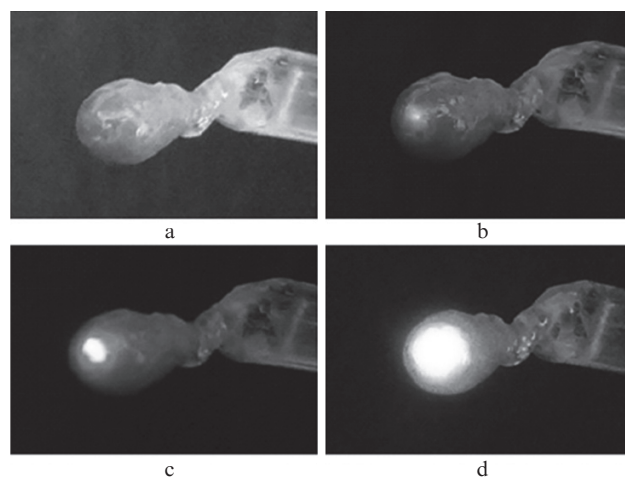
Figure 2. Er_2O_3 polycrystalline sample on a quartz rod 3 mm in diameter (a) and transformation of its emission intensity distribution in the visible region spaced by 3–5 s after switching on of a CO_2 laser with a power of $\sim$2 W (b–d).

intensity distribution on a sample after stepwise switching on of laser radiation. Heating of the sample by absorbed radiation in the region of a laser spot smaller than 1 mm in diameter is accompanied by an increase in the emission area and intensity, as well as by a change in the emitting surface colour from red to yellow and then to white. Deep under the face surface, the sample is heated to a lower temperature due to a low thermal conductivity. The emission of Er_2O_3 polycrystals ceases approximately one second after cutting off the laser beam.

4. The reflection and emission spectra of Er_2O_3 in the regions of 300–1100 and 1100–1700 nm were recorded by AvaSpec-2048 and NIR128-1.7-RS232 fibre-coupled spectrometers. Figures 3a, 3b show the reflection spectra of Er_2O_3 polycrystals synthesised by laser heating (the absorption bands in the visible and near-IR spectral regions are denoted by the corresponding terms of the excited electronic states of Er^{3+} ions).

The emission spectra of Er_2O_3 polycrystals in the range 400–1700 nm were studied upon stepwise switching on (Figs 3c, 3d) and off (inset in Fig. 3c) of a repetitively pulsed CO_2 laser with an average power of ~2 W. The figures show the times of recording of the spectra.

The SE spectra of Er_2O_3 polycrystals in the range 1100–1700 nm in Fig. 3d consist of bands in the region of the $^4I_{13/2} \rightarrow {}^4I_{15/2}$ transitions with the maxima at $\lambda \approx 1475$, 1545, and 1640 nm, which correspond to the absorption spectra in Fig. 3b. The shape of the spectra almost does not change as the laser radiation intensity increases by ~250 times and is similar to the luminescence spectra of impurity oxides
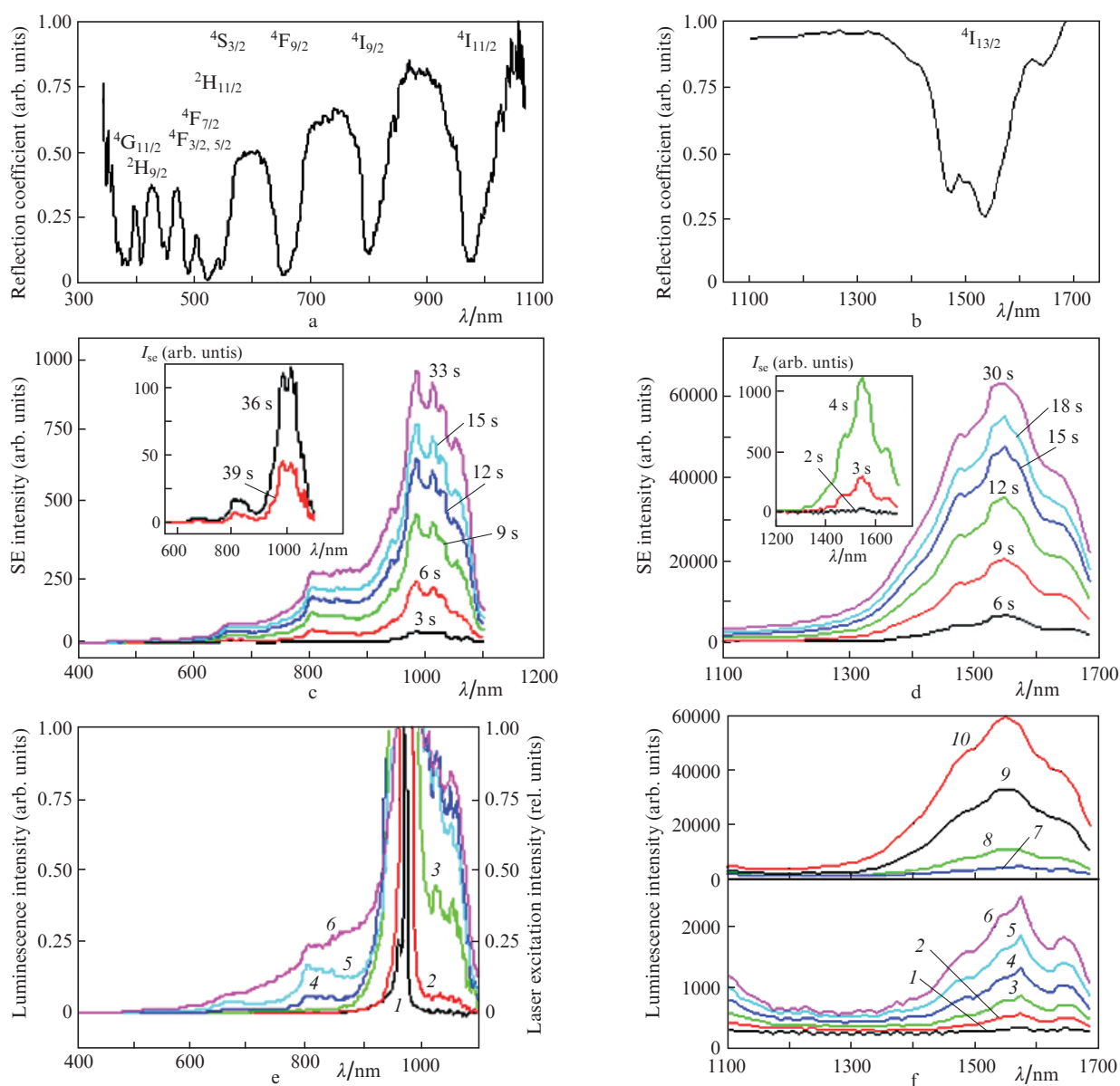
Figure 3. Reflection spectra of Er_2O_3 polycrystals (a, b), SE spectra of Er_2O_3 polycrystals at the $^4F_{9/2}$, $^4I_{9/2}$, $^4I_{11/2}$, $^4I_{13/2} \rightarrow {}^4I_{15/2}$ transitions at different time moments (figures at the curves) upon stepwise switching on (c, 3–33 s; and d) and off (c, 36–39 s) of laser-thermal excitation, excitation spectra of the $^4I_{11/2}$ level of Er^{3+} ions at $\lambda \approx 975$ nm at the laser excitation intensity $I_{las} \approx 48$ W cm^{-2} (*1*) and luminescence spectra of the $^4I_{11/2} \rightarrow {}^4I_{15/2}$ transitions at $I_{las} = 6320$ (*2*), 8000 (*3*), 9600 (*4*), 13120 (*5*), and 16000 W cm^{-2} (*6*) (e), and luminescence spectra of the $^4I_{13/2} \rightarrow {}^4I_{15/2}$ transitions at $I_{las} \approx 112$ (*1*), 456 (*2*), 800 (*3*), 1160 (*4*), 1560 (*5*), 1920 (*6*), 2320 (*7*), 3040 (*8*), 3840 (*9*), and 4320 W cm^{-2} (*10*) (f).

$Er^{3+}:SiO_2$ and $Er^{3+}:Al_2O_3$ [1, 22]. The intensity of SE bands is some orders of magnitude higher than the intensity of the equilibrium TR of the crystal lattice (pedestal).

The dependence of the SE spectra of Er_2O_3 polycrystals in the range 400–1100 nm on the laser heating duration was studied using an AvaSpec-2048 spectrometer by the same method. The spectra were recorded upon stepwise switching on and off of the CO_2 laser. The spectrometer sensitivity was corrected by the TR spectrum of a reference tungsten lamp. The recorded SE spectra (Fig. 3c) consist of broad weakly structured bands of the $^4F_{9/2}$, $^4I_{9/2}$, $^4I_{11/2} \rightarrow {}^4I_{15/2}$ transitions corresponding to the absorption spectra of Er^{3+} in Er_2O_3 polycrystals. From the SE spectra, one can conclude that the change of the target colour from red to yellow with changing the laser radiation intensity is caused by mixing of the spectral bands at $\lambda = 660$ and 530 nm. According to [20], the spectral selectivity is retained up to 1873 K.

The luminescence spectra of Er_2O_3 polycrystals in the range 1100–1700 nm (Fig. 3f) were studied under resonant excitation of the $^4I_{11/2}$ level of Er^{3+} ions by cw radiation of a fibre coupled (core diameter 400 μm) laser diode array with the power $P_{las} < 20$ W at $\lambda \approx 975$ nm. The radiation power was varied by the array current. Figure 3f shows the luminescence spectra of Er^{3+} ions in Er_2O_3 polycrystals corresponding to the $^4I_{13/2} \rightarrow {}^4I_{15/2}$ transitions at different intensities I_{las} of resonant laser excitation of the $^4I_{11/2} \leftarrow {}^4I_{15/2}$ transitions at $\lambda \approx 975$ nm. The shapes of the SE and luminescence bands of Er_2O_3 polycrystals almost coincide in the entire region of excitation intensities. An exception is the luminescence peak at $\lambda = 1570$ nm and $I_{las} \leqslant 2000$ W cm^{-2}. As the excitation power P_{las} increases by a factor of ~40, the intensity of the luminescence peak at $\lambda \approx 1550$ nm increases by ~250 times (Fig. 3f) and is interpolated by the formula $I_{max} = 212\exp(P_{las}/0.97) + 76$. The nonlinear intensity increase in this region of the luminescence spectrum is obviously related to an additional thermal multiphonon excitation of the $^4I_{13/2}$ level due to increasing temperature.

The luminescence spectra of Er_2O_3 polycrystals in the region of 400–1100 nm were studied upon similar excitation of the $^4I_{11/2}$ level of Er^{3+} ions by the same diode laser array. Figure 3e shows the spectra of pump radiation (1) and luminescence of Er_2O_3 polycrystals ($2–6$) at different laser radiation intensities. The resonant luminescence line at $\lambda = 975$ nm is subtracted from the spectra for demonstration of compo-

nents with lower intensities. At the laser excitation intensity $I_{las} \leqslant 8$ kW cm^{-2}, the spectra contain only the Stokes components [Fig. 3e, curves (2) and (3)] with respect to the $^4I_{11/2} \rightarrow {}^4I_{15/2}$ luminescence excitation spectrum [Fig. 3e, curve (1)]. At higher excitation intensities, the spectra also show anti-Stokes bands corresponding to the SE at the $^4I_{9/2} \rightarrow {}^4I_{15/2}$, $^4F_{9/2} \rightarrow {}^4I_{15/2}$, and $^2H_{11/2}$, $^4S_{3/2} \rightarrow {}^4I_{15/2}$ electronic-vibrational transitions of Er^{3+} ions [Fig. 3e, curves (4) and (5)] due to an increase in the sample temperature. Further increase in the excitation intensity is accompanied by a decrease in the intensity of these transitions with respect to the TR pedestal of the crystal lattice.

Let us compare the experimental SE spectra of Er_2O_3 polycrystals at low and high temperatures. The SE spectra of Er_2O_3 polycrystals in the range 300–1100 nm (Fig. 4a) are measured with the highest possible sensitivity of the AvaSpec-2048 spectrometer without sensitivity correction. At a small reversible variation in the intensity of laser-thermal excitation with a repetition rate exceeding 1 Hz, the Er^{3+} spectra (shifted along the ordinate axis in Fig. 4a for clearness) appear as luminescence bursts on the background with unchanged shape of electronic-vibrational SE bands.

At the sample surface temperature higher than 1500 K, the selectivity of spectra decreases due to an increase in the emissivity of the continuous spectrum of the crystal lattice [20], and the laser spot becomes white. The shape of the normalised experimental spectrum of the Er_2O_3 laser melt [Fig. 4b, curve (1)] is close to the calculated TR spectrum of a blackbody [Fig. 4b, curve (2)] at $T = T_m$. The minima of the laser melt spectrum correspond to the Er_2O_3 absorption bands in Fig. 3a and are explained by the self-absorption of Er^{3+} radiation in the cooler regions of the samples.

5. It is experimentally found that the Er_2O_3 samples synthesised by laser heating have a dense cubic microcrystalline structure with the lattice constant $a = 10.5637(7)$ Å [27]. The temperature resistance of oxide samples on a quartz substrate under the extremal conditions of synthesis and hypersonic aerodynamics [14] is related to the microstructure of the interface at which the laser welding causes a chemical reaction with formation of the erbium silicate phase Er_2SiO_5.

The colour of Er_2O_3 polycrystals heated by a quasi-cw laser is determined by the steady-state temperature distribution formed in the processes of multiphonon and electronic-vibrational relaxation of laser energy absorbed by the crystal
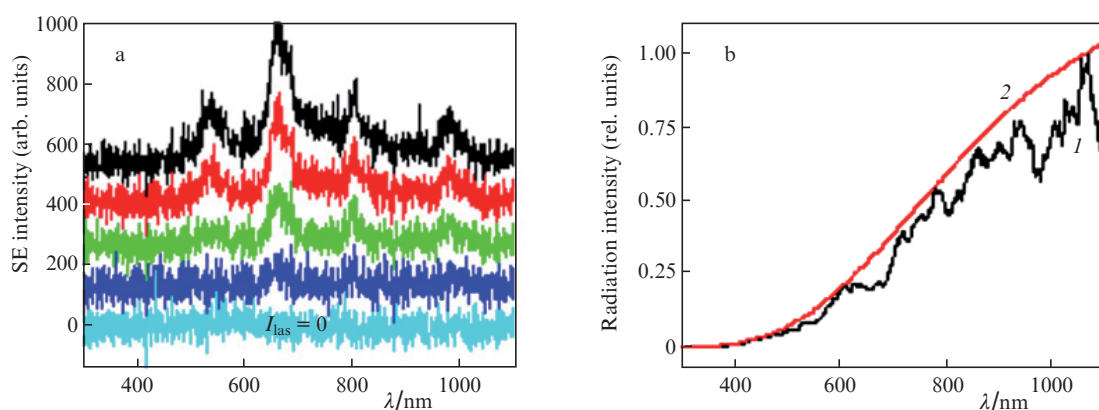
Figure 4. SE spectra of Er_2O_3 polycrystals near the detection threshold at different laser-thermal excitation intensities (a), as well as normalised spectra of Er_2O_3 laser melt (1) and a blackbody (2) at $T_m = 2691$ K (b).

lattice and depends on the heat conduction and self-radiation. The local radiation spectrum of Er_2O_3 samples in the range 400–1700 nm is a superposition of the SE spectra of electronic-vibrational transitions of Er^{3+} ions and the TR of the crystal lattice. The relative SE and TR intensities are determined by the local temperature-dependent emissivity of the Er^{3+} electronic states $J_{se}(\lambda, T)$ and the crystal lattice $J_{cl}(\lambda, T)$.

In the process of heating of Er_2O_3 polycrystals, the SE spectral bands arise on the background as bursts of luminescence. The SE spectra of Er_2O_3 polycrystals in the range 400–1700 nm at $T < 1400$ K correspond to the absorption spectra of Er^{3+} ions and their shape is almost independent of temperature. The intensity of SE bands of Er_2O_3 polycrystals in the quasi-cw regime is many times higher than the TR pedestal intensity because $J_{se} \gg J_{cl}$ and J_{se} changes synchronously with the laser radiation intensity. In this case, the SE of Er_2O_3 polycrystals upon laser-thermal excitation of their surface is a thermodynamically nonequilibrium process. In this temperature region, the SE is identical to the luminescence of Er^{3+} ions, the possibility of which under thermal (multiphonon) excitation was discussed in [28]. The luminescence spectra of Er_2O_3 polycrystals under intense laser excitation of the $^4I_{11/2}$ level of Er^{3+} ions are similar to the SE spectra. The anti-Stokes luminescence bands of Er^{3+} ions are explained by the appearance of additional SE caused by heating of the crystal matrix due to multiphonon relaxation. A difference between the SE and luminescence spectra is observed at low temperatures and low resonant laser excitation intensities, when only the Stokes luminescence occurs. A similar transformation of the SE and luminescence spectra of Yb_2O_3 polycrystals was studied in [26], while the cathodoluminescence and SE of Er_2O_3 oxides and Er^{3+}:YAG crystals upon electron beam excitation was considered in [29].

In the region of $T = 1540–1873$ K, the emissivities of the SE and the TR pedestal are comparable, $J_{se} \approx J_{cl}$. At $T \approx T_m = 2691$ K, the condition $J_{se} < J_{cl}$ is fulfilled and the emissivity of the Er_2O_3 melt becomes closer to the blackbody emissivity J_{bb}. Note that the saturation of the SE intensity with increasing laser excitation intensity occurs due to a phase transition near the melting temperature of Er_2O_3 [23].

The temperature dependences of the SE and luminescence spectra of Er_2O_3 polycrystals upon laser-thermal and resonant laser excitation testify to the fundamental role of the interaction of the electronic $^4f_{11}$ shell of Er^{3+} ions with intrinsic vibrations of the crystal lattice in the process of multiphonon radiative and nonradiative relaxation.

The energy balance upon laser heating of Er_2O_3 polycrystals in the stationary case is described by the relation

$$(1 - r)I_{las}S = P_h + P_{se} + P_t,$$

where r is the laser radiation reflection coefficient, S is the laser beam cross section, and P_h, P_{se}, and P_t are the powers of heat losses, selective emission, and continuous radiation of the target. A decrease in P_h is accompanied by an increase in the coefficient of absorbed energy conversion into the target emission. The energy efficiency of SE and TR in Er_2O_3 polycrystals is characterised by the temperature-dependent emissivities of Er^{3+} ions J_{se} and crystal lattice J_{cl}. At low temperatures, $J_{se} \gg J_{cl}$ and $P_{se} \gg P_t$. With increasing temperature, P_t increases faster than P_{se}, and the shape of the integral spectrum of Er_2O_3 becomes closer to the shape of the blackbody spectrum. The temperature dependence of the J_{se} and J_{cl} ratio is obviously caused by the quantum nature of the corresponding radiative transitions.

The time dependences of the intensities of the SE spectral bands in the range 400–1100 nm and of the central SE maximum at $\lambda \approx 1545$ nm (Fig. 5) upon stepwise switching on and off of the CO_2 laser testify that the population of energy levels depends on the electron temperature $T_e = T$ stable at the given time scale, i.e., point to the thermal excitation of Er^{3+} ions. The shape of the leading edges of the SE intensity is interpolated by the formula $I \approx 10^3\{1 - [1 + (t/10)^3]^{-1}\}$. The SE intensity decay is exponential with the time constant $\tau \approx 1$ s. The smooth rise and the steep fall of the SE of Er_2O_3 polycrystals upon the stepwise switching on and off of laser radiation are determined by a power balance of heating with thermal and radiative losses.

The synthesis of rare-earth samples with variable chemical composition by laser heating is promising for efficient investigations of the microstructure, spectral-kinetic, and thermophysical properties of models of different forms and for applications in quantum electronics, microelectronics, thermophotovoltaics, and hypersonic aerodynamics.
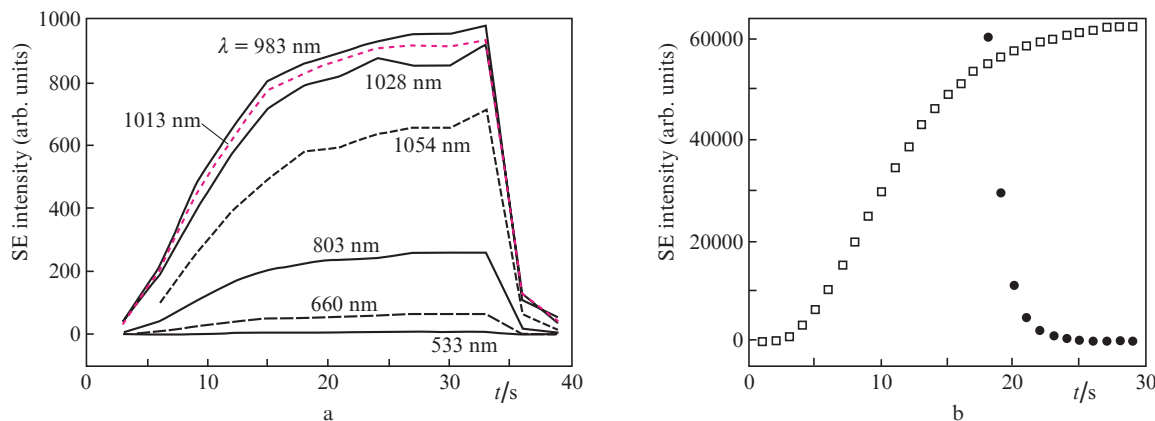
Figure 5. Time dependences of the intensity of SE spectral bands at $\lambda = 533–1028$ nm upon stepwise switching on and off of the CO_2 laser (a) and SE intensities at $\lambda \approx 1545$ nm upon stepwise switching on ($\square$) and off ($\bullet$) of laser radiation (b).

References

1. Miritello M., Lo Savio R., Piro A.M., Franzò G., Priolo F., Iacona F., Bongiorno C. *J. Appl. Phys.*, **100**, 013502 (2006).
2. Michael C.P., Yuen H.B., Sabnis V.A., Johnson T.J., Sewell R., Smith R., Jamora A., Clark A., Semans S., Atanackovic P.B., Painter O. *Opt. Express*, **16**, 19651 (2008).
3. Savchyn O., Todi R.M., Coffey K.R., Kik P.G. *Appl. Phys. Lett.*, **93**, 233120 (2008).
4. Savchyn O., Todi R.M., Coffey K.R., Kik P.G. *Appl. Phys. Lett.*, **94**, 241115 (2009).
5. Kamineni H.S., Kamineni V.K., Moore R.L. II, Gallis S., Diebold A.C., Huang M., Kaloyeros A.E. *J. Appl. Phys.*, **111**, 013104 (2012).
6. Phung T.H., Srinivasan D.K., Steinmann P., Wise R., Yu M.-B., Yeo Y.-C., Chunxiang Z. *J. Electrochem. Soc.*, **158**, H1289 (2011).
7. Licciulli A., Diso D., Torsello G., Tundo S., Maffezzoli A., Lomascolo L., Mazzer M. *Semicond. Sci. Technol.*, **18**, S174 (2003).
8. Bitnar B., Durisch W., Palfinger G., Von Roth F., Vogt U., Brönstrup A., Seiler D. *Semiconductors*, **38**, 980 (2004).
9. Chubb D.L. *Fundamentals of Thermophotovoltaic Energy Conversion* (Amsterdam, Netherlands, Boston, Oxford, UK: Elsevier, 2007).
10. Teofilo V.L., Choong P., Chang J., Tseng Y.L., Ermer S. *J. Phys. Chem. C*, **112**, 7841 (2008).
11. Pint B.A., Tortorelli P.F., Jankowski A., Hayes J., Muroga T., Suzuki A., Yeliseyeva O.I., Chernov V.M. *J. Nucl. Mater.*, **329–333**, 119 (2004).
12. Hishinuma Y., Murakami S., Matsuda K., Tanaka T., Tasaki Y., Tanaka T., Nagasaka T., Sagara A., Muroga T. *Plasma Fusion Res., Special Issue 1*, **7**, 2405127 (2012).
13. Tsisar V., Yeliseyeva O., Muroga T., Nagasaka T. *Plasma Fusion Res., Special Issue 1*, **7**, 2405123 (2012).
14. Alferov V.I., Marchenko V.M. *Teplofiz. Vysokikh Temp.*, **50**, 550 (2012).
15. Kasuya A., Suezawa M. *Appl. Phys. Lett.*, **71**, 2728 (1997).
16. Chen K.M., Saini S., Lipson M., Duan X., Kimerling L.C. *Proc. SPIE Int. Soc. Opt. Eng.*, **4282**, 168 (2001).
17. Golovlev V.V., Chen C.H.W., Garrett W.R. *Appl. Phys. Lett.*, **69**, 280 (1996).
18. Krishna M.G., Biswas R.G., Bhattacharya A.K. *J. Phys. D: Appl. Phys.*, **30**, 1167 (1997).
19. Torsello G., Lomascollo M., Licciulli A., Diso D., Tundo S., Mazzer M. *Nature Mater.*, **3**, 632 (2004).
20. Guazzoni G.E. *Appl. Spectrosc.*, **26**, 60 (1972).
21. Seat H.C., Sharp J.H. *Meas. Sci. Technol.*, **14**, 279 (2003).
22. Bufetova G.A., Kashin V.V., Nikolaev D.A., et al. *Kvantovaya Elektron.*, **36** (7), 616 (2006) [*Quantum Electron.*, **36** (7), 616 (2006)].
23. Marchenko V.M. *Laser Phys.*, **17**, 1146 (2007).
24. Marchenko V.M. *Laser Phys.*, **20**, 1390 (2010).
25. Marchenko V.M. *Laser Phys.*, **21**, 383 (2011).
26. Marchenko V.M., Iskhakova L.D., Kir'yanov A.V., Mashinsky V.M., Karatun N.M., Sholokhov E.M. *Laser Phys.*, **22**, 177 (2012).
27. Zinkevich M. *Prog. Mater. Sci.*, **52**, 597 (2007).
28. Adirovich E.I. *Usp. Fiz. Nauk.*, **40**, 341 (1950).
29. Marchenko V.M., Voitik M.G., Yuryev V.A. *Laser Phys.*, **18**, 756 (2008).